

BRIEF COMMUNICATION

AN EXAMPLE OF THE APPLICATION OF THE BOUNDING DRYOUT CRITERIA IN HORIZONTAL STEAM-GENERATING TUBES FOR THE CASE OF CIRCUMFERENTIALLY NONUNIFORM HEAT FLUX

Z. RUDER and A. BAR-COHEN

Mechanical Engineering Department, Ben-Gurion University of the Negev, Beer Sheva, Israel

P. GRIFFITH

Mechanical Engineering Department, MIT, Cambridge, MA 02139, U.S.A.

(Received 29 May 1985; in revised form 11 November 1985)

1. INTRODUCTION

Recently, semianalytical dryout criteria for horizontal steam-generating tubes operating within the low- and moderate-quality ranges were presented by Bar-Cohen *et al.* (1984, 1986). It was shown that not only the stratified flow pattern, but also segments of the intermittent and dispersed bubble flow patterns may, under certain operating and geometric conditions, result in tube overheating.

The local circumferential tube nonisothermality within the moderate-quality range (x up to about 0.5–1%), in the intermittent flow pattern, was shown to result from the insufficiently high slug formation/passage frequency which would yield the evaporation of the thin liquid film on the top of the tube by an externally applied heat flux. To avoid this phenomena of the *inlet* slug dryout the liquid velocity at the tube inlet was recommended to be

$$U_L > 10^5 d \left(\frac{q''}{h_{LG} \rho_L} \right)^{0.833} \quad [1]$$

or, in dimensionless form:

$$Fr_L > 3.2 \cdot 10^4 d^{0.5} \left(\frac{q''}{h_{LG} \rho_L} \right)^{0.833} \quad [1a]$$

In these expressions U_L is the superficial liquid velocity, d is the tube internal diameter, q'' is the externally applied heat flux, h_{LG} is the latent heat, ρ_L is the liquid density and Fr_L is the liquid superficial velocity-based Froude number.

As for the dispersed bubble flow pattern, it was shown that the low-quality (x up to 0.025–0.05%) circumferential nonisothermality may be a result of two different events. First, the tube inlet geometry (bends, fittings etc.) gives rise to a stationary “vapor bubble” occupying the top of the tube. Second, the very genesis of the intermittent (slug) flow pattern brings about the appearance of a locally-stratified zone. This zone, associated with the diabatic transition between the intermittent and dispersed bubble patterns, works like a “piston” producing new consecutive slugs. It was recommended on an experimental and analytical basis (Ruder *et al.* 1984) that when the calming section of a horizontal tube is long,

$$\frac{L_{\text{calm}}}{d} > 90;$$

the criterion to avoid the lower quality top overheating is

$$U_L > \sqrt{gd} \quad [2]$$

or, in dimensionless form:

$$Fr_L > 1. \quad [2a]$$

If, alternatively, the calming section is short,

$$\frac{L_{\text{calm}}}{d} < 90$$

and the fittings (especially those whose internal diameter is less than that of the tube) precede the bend. It was experimentally found that

$$U_L > 2\sqrt{gd} \quad [3]$$

or, in dimensionless form:

$$Fr_L > 2. \quad [3a]$$

In the expressions given above L_{calm} is the length of the straight, unheated tube calming section.

The termination of the moderate-quality nonisothermality was shown to correspond to the hydrodynamic transition from the intermittent to annular flow. The dimensionless criterion defining this transition was shown (Weisman *et al.* 1973; Bar-Cohen *et al.* 1984) to be

$$Fr_G = (gd)^{1.327} \left\{ \frac{1.9[g(\rho_L - \rho_G)\sigma]^{0.05}}{U_L^{0.125} \rho_G^{0.1}} \right\}^{3.607} \quad [4]$$

where the superficial gas velocity-based Froude number is defined as

$$Fr_G = \frac{U_G}{\sqrt{gd}}. \quad [4a]$$

In [4] and [4a], U_G is the gas superficial velocity, ρ_G is the gas density and σ is the surface tension.

All the aforementioned isothermality bounding criteria [1a]–[4a] can be graphically expressed on the diabatic flow regime map, as shown in figure 1. These criteria were verified

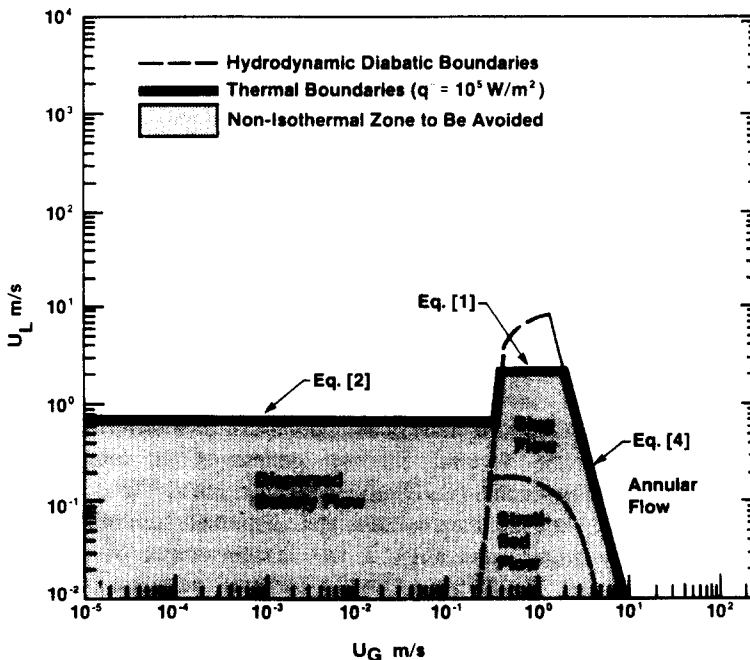


Figure 1. Typical thermal/hydrodynamic map for a horizontal tube.

using various data available in the literature for the case of circumferentially uniform heat flux, which resulted in the overheating of *the top* of the tube (Bar-Cohen *et al.* 1984).

Although most of the literature data are associated with uniformly-heated boiler tubes, most practical applications of modern boilers and evaporators include circumferentially (and often axially) nonuniform external heat loading. The striking example of the latter case is fluidized-bed combustor boilers, generally characterized by the high extent of nonuniformity of both hydrodynamics inside the bed and bed/tube transfer (e.g. Chandran *et al.* 1979). For a fluidized bed operating in a bubbling regime, the lowest values of the external bed/tube heat transfer coefficients may be expected to occur on top of the pipe, being associated with the so-called stationary "particle cap" at this location. Provided that the fluidizing medium (e.g. air) is distributed uniformly, the highest h_{out} -values generally correspond to the side and near the center of the pipe where particle motion is most vigorous. The location of tube overheating appears, hence, to be circumferentially shifted to the side or even down to the bottom.

In the present study, experimental results related to such a peculiar, "shifted overheating" phenomena are interpreted by means of the "thermal" criteria [1]–[4] which are applied to the case of an extremely nonuniform externally-imposed heat flux and unfavorable tube entrance conditions. The study represents, thus, a practical effort to extend and further validate the approach developed and verified previously for uniform heating to the case of nonuniform heating.

2. EXPERIMENTAL APPARATUS

The experimental apparatus is described in detail by Ruder (1984). Briefly, a horizontal 0.0254 m i.d. test pipe, instrumented with 18 thermocouples axially arranged in the wall so as to form three measuring stations, was immersed in an ambient temperature, large-particle, bubbling, air-fluidized bed, 61 × 61 cm in size. While the R-22 two-phase mixture flowed through the pipe, the circumferential wall temperature profiles were measured and internal heat transfer coefficients were calculated.

For the reported conditions, the ratio of the length of the entrance section of the pipe, preceded by a horizontal/vertical bend, to its internal diameter was $\ll 90$. Furthermore, this straight section between the bend and the test pipe inside the fluidized bed was usually used for circumferentially uniform preheating, thus altering the hydrodynamic phenomena in the tube which, hence, had no possibility of developing from the inlet.

The external bed/tube heat transfer coefficients were found to be both circumferentially and axially nonuniform (figure 2), which was a result not only of the usual hydrodynamic phenomena in the bed but also of the nonuniform distribution of fluidizing air (Bar-Cohen

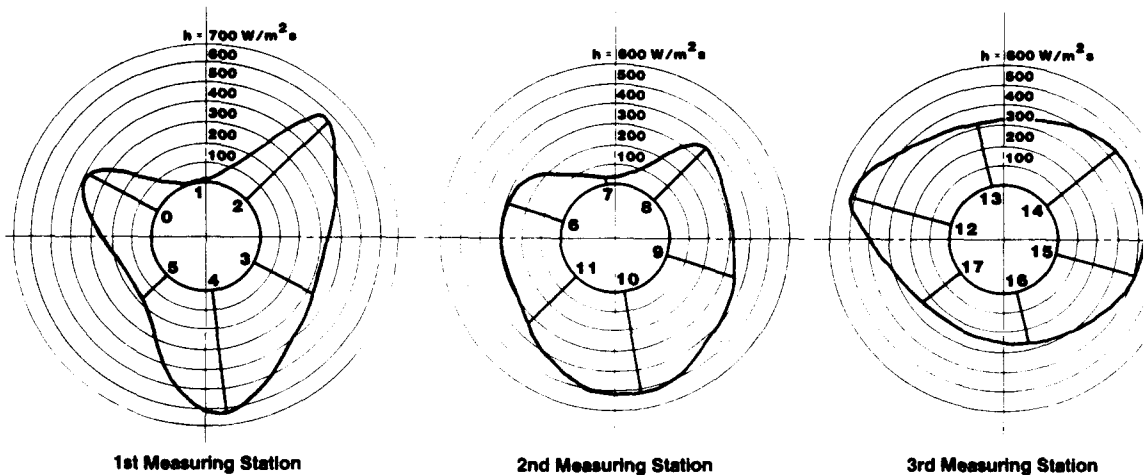


Figure 2. Fluidized bed/pipe local heat transfer coefficient circumferential and axial distribution.

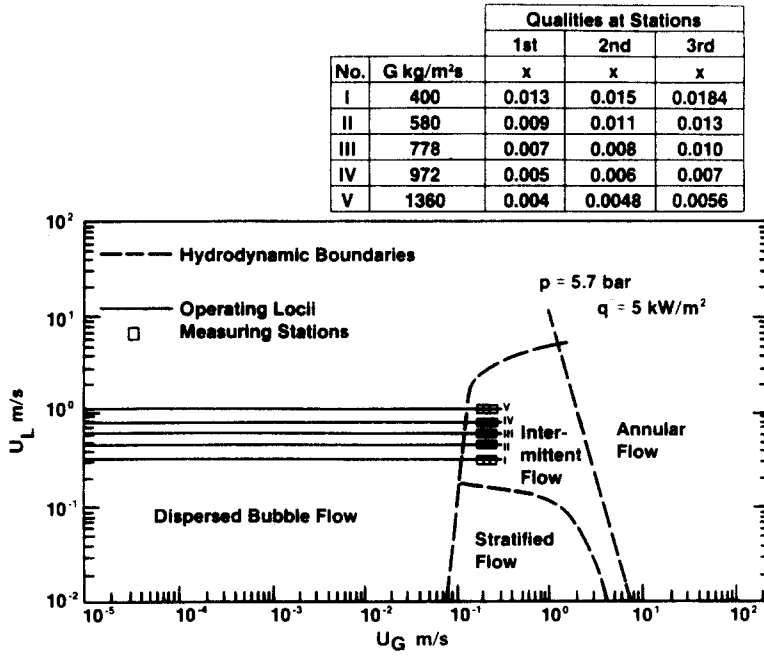


Figure 3. A typical flow regime map for the operating conditions of the fluidized bed model, R-22-carrying experimental apparatus.

et al. 1983). The lowest value of h_{out} was found on top of the pipe, whereas the highest h_{out} -values were obtained at the side and near the center of the pipe (figure 2).

A typical flow pattern map for the operating conditions of the R-22/FBC apparatus is presented in figure 3. For the specified conditions, when the mass flow rates were higher than approx. 220 kg/m² s, the test tube was operating in the intermittent pattern.

In the absence of R-22 preheating, the right-hand end of the various loci on the map (figure 3) correspond to the liquid and vapor superficial velocities prevailing at the third axial station along the test section. While preheating did not, of course, alter the location of the hydrodynamic boundaries on the maps, it did directly influence the quality and superficial velocities associated with a specified mass flux at every location in the test section.

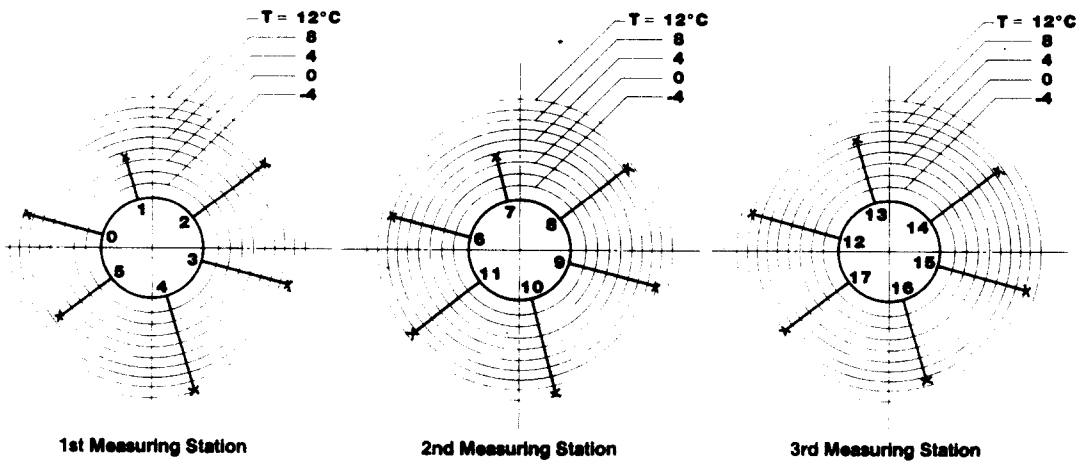


Figure 4a. Typical wall temperature circumferential distribution for the R-22-carrying test section stratified flow.

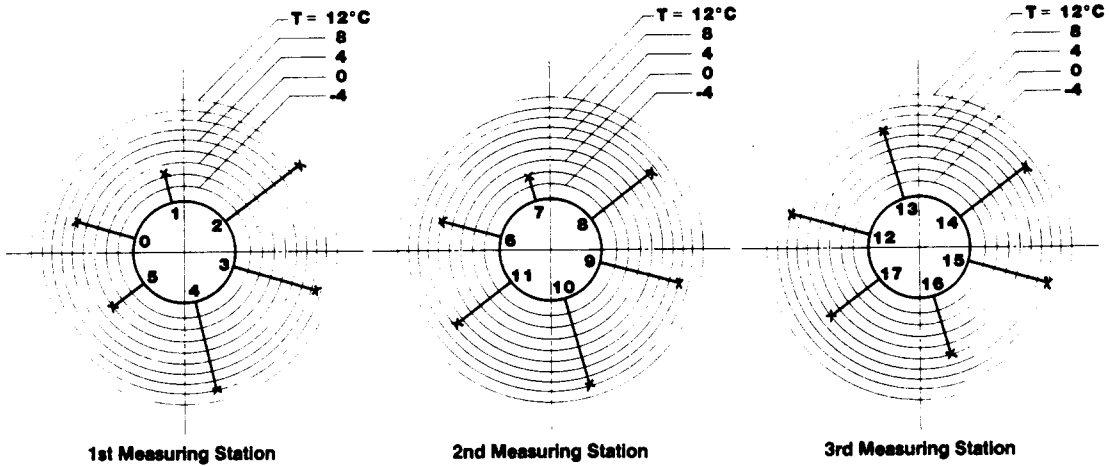


Figure 4b. Typical wall temperature circumferential distribution for the R-22-carrying test section stratified flow.

3. EXPERIMENTAL RESULTS

A typical, empirically obtained, circumferential temperature distribution for the R-22 test section in the fluidized bed is displayed in figures 4a,b. As may be seen, the temperature at the top of the tube was the lowest at each of the three measuring stations along the pipe for both the stratified and intermittent flow patterns. This result seems to be associated with the low external heat transfer coefficient at this location, which leads to a locally reduced heat flux. Since in the fluidized bed/R-22 experiments the influence of the two-phase flow pattern on the circumferential temperature difference was, interestingly, masked by the variation in the *external* heat transfer coefficients, attention must be turned directly to the behavior of the *internal* heat transfer coefficients for the conditions of interest.

For the *stratified* flow (figure 5), the empirical h_{in} obtained at the top of the pipe was, typically, surprisingly high, both in absolute terms and relative to lower points on the pipe. This result can be explained by the occurrence of evaporative heat transfer, through a relatively thin liquid film remaining at the top of the pipe at this location. This film originates, no doubt, at the inlet of the pipe and, due to the very low locally-imposed heat flux, appears to remain in existence at least up to approx. 0.6 m downstream. It may be anticipated that evaporation will reduce the thickness of this film and lead to progressively

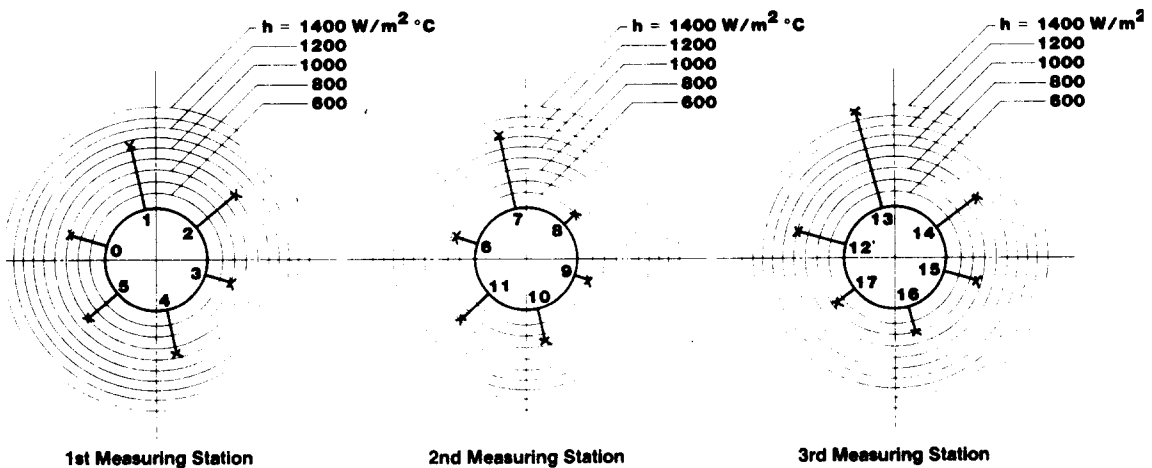


Figure 5. Typical internal heat transfer coefficient circumferential profiles for the case of stratified flow in the R-22-carrying test section.

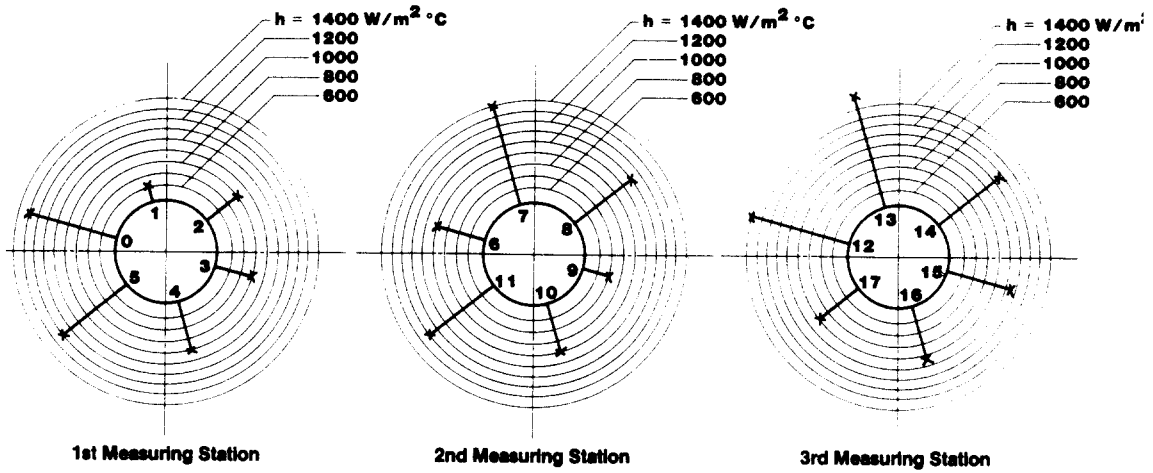


Figure 6. Typical internal heat transfer coefficient circumferential profiles for the case of stratified flow in the R-22-carrying test section.

higher heat transfer coefficients in the axial direction until complete film dryout occurs. This trend, without dryout, is in clear evidence in the data plotted in figure 5.

The *intermittent* flow pattern, usually resulting in the moderate-quality dryout, also displayed certain peculiarities in this particular case. Based on the flow regime maps, R-22 mass fluxes above $220 \text{ kg/m}^2 \text{ s}$ were sufficient to avoid the occurrence of the stratified flow in the horizontal test section. Indeed, R-22 mass fluxes in excess of this value displayed distinct similarities in their axial and circumferential h_{in} variation, including certain "dynamic" characteristics, and notable differences with the h_{in} variation observation at lower mass fluxes.

In particular, near the test section inlet, h_{in} at the top was found to be either the lowest or among the lowest, of the circumferential values (figure 6). As can be seen in the relevant flow regime maps (e.g. figure 3), the conditions at two stations further downstream, for R-22 mass fluxes above $220 \text{ kg/m}^2 \text{ s}$, place these sites in the intermittent flow pattern. For most of the cases at both the second and third measuring stations, h_{in} at the top of the pipe was among the highest.

At the second measuring station, the maximum heat flux was applied to the bottom but the internal heat transfer coefficients at this particular spot exhibited no considerable decrease (figure 6). At the third station along the tube, the h_{in} -values were found to be highest at the side.

The complex dynamics of the instantaneously measured heat transfer coefficients while operating in the intermittent flow pattern are described in detail by Bar-Cohen *et al.* (1983).

4. ANALYSIS—APPLICATION OF THE LOCAL DRYOUT CRITERIA TO THE PRESENT EXPERIMENTAL RESULTS

It is convenient to use a "thermal map" corresponding to the operating and geometric conditions under investigation to analyze the results obtained. Such a map is shown in figure 7 which is a "thermal" modification of the hydrodynamic map represented in figure 3. In figure 7 the area where U_L -values and U_G -values are associated with tube circumferential nonisothermality (shaded zone), is separated from the zone characterized by the tube isothermal operation by means of bounding criteria [3], [1] and [4]. The short section connecting the low-quality thermal boundary [3] with the moderate-quality thermal boundary [1] is seen to coincide with the diabatic hydrodynamic transition between the dispersed bubble and intermittent (slug) flow patterns, as was shown in detail by Bar-Cohen *et al.* (1986) and Ruder (1984). The operating loci corresponding to various water mass flow rates (see table in figure 3) are redrawn in figure 7 which makes it possible to easily compare the results obtained with the isothermality bounding criteria.

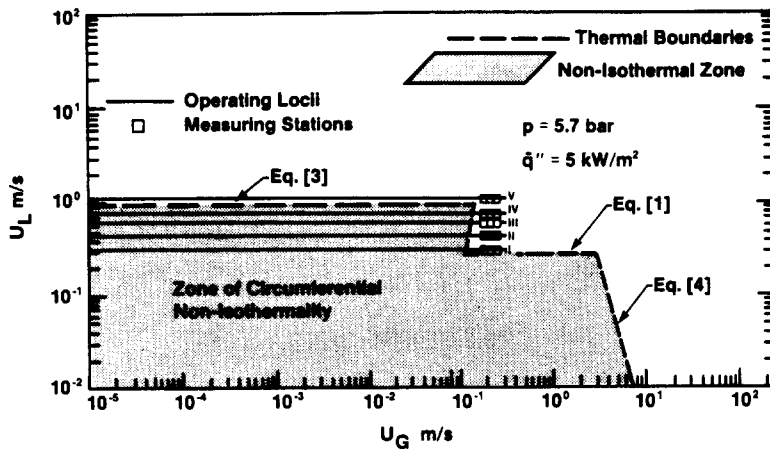


Figure 7. Thermal map for the operating conditions of the fluidized bed/R-22 experiments. For the exact operating values of R-22 mass flow rates and vapor qualities at different measuring stations—see the table in figure 3.

The results obtained for the top of the first measuring station are reminiscent of the low-quality nonisothermal zone identified in the water/steam results by Bar-Cohen *et al.* (1984, 1986) and shown by these authors to be associated with various entrance effects. Moreover, since in this particular case the calming section is short, criterion [2] cannot be expected to represent the correct thermal boundary for the low-quality region. At the same time, [3], interestingly, does appear to be the bounding criterion for the present case. Actually, $Fr_L = 2$ yields the bounding inlet R-22 velocity value, for low qualities, to equal about 1 m/s. Accounting for the general imprecision of the thermal criteria, which is about $\pm 25\%$ (Ruder 1984), this would explain low h_{in} -values for all operating mass fluxes falling in the range of 220–1360 kg/m² s (figure 7).

Returning to the moderate-quality boundary, i.e. [1], and remembering that in the case of a *nonuniform heat flux* only *local* values of q'' are relevant (Ruder *et al.* 1984), the high values of the tube internal heat transfer coefficients obtained at the top could easily be predicted. Actually, putting into the calculations the correct values of local top heat fluxes (1300 W/m² for the second measuring station and 5400 W/m² for the third one), would lead the “critical” Fr_L numbers to be 0.2 and 0.6, respectively, or to bounding U_L -values of 0.1 and 0.3 m/s, respectively. All this would mean that the operating mass flow rates of 220–1360 kg/m² s were high enough to prevent complete evaporation of the thin R-22 liquid film at the top in between slugs for the heat fluxes of interest.

Graphically, the operating loci on the flow maps (figure 7) lie above the nonisothermal moderate-quality region and there is, thus, no possibility for low h_{in} -values on the top for all operating mass flow rates. On the contrary, due to the continuous evaporating process, the h_{in} -values on the top are rather high (figure 6).

For the locally maximum heat fluxes, the results would also appear quite explainable. At the second measuring station, the peak of the heat flux (10.6 kW/m²) was applied to the bottom of the tube where there was more liquid than elsewhere. Yet, unless this local heat flux exceeds the critical heat flux in boiling, the local dryout at this spot could not be expected to occur (figure 6). At the third station along the tube, the maximum heat loading (12 kW/m²) was at the side. The imposition of $h_{out max}$ is seen in figure 2 to be at the vertical position of 0.55–0.7*d*. Interestingly, the “minimum” liquid level in the tube calculated according to the approach suggested previously by Ruder *et al.* (1984) also falls within this range, reaching the value of 0.6*d* for the highest mass flow of 1360 kg/m² s; 0.55*d* for $G = 972$ kg/m² s; 0.5*d* for $G = 778$ kg/m² s; 0.42*d* for $G = 580$ kg/m² s and 0.35*d* for $G = 440$ kg/m² s. It, thus, follows that the internal heat transfer coefficients found to be the highest at this particular spot result from the constant evaporative processes. Were the liquid level lower, h_{in} -values could be expected to be very low at this particular measuring point.

5. CONCLUSIONS

The method of predicting the low- and moderate-quality dryout in horizontal boiler tubes, previously proposed for circumferentially uniform heat loading, has been applied to the case of nonuniform heat fluxes encountered in practical applications. It has been demonstrated for the empirical results of fluidized bed/R-22 heat transfer that the thermal bounding criteria and the recommended method of calculating the minimum liquid level in the pipe described earlier are applicable to the latter case provided that the local thermal parameters are accounted for.

REFERENCES

- BAR-COHEN, A., GRIFFITH, P., RUDER, Z., KLEIN, Y. & SCHWEITZER, H. 1983 Flow boiling in inclined tubes in fluidized bed combustors. Final Report TPL 002/83 to the US/Israel Bi-National Science Foundation, Mechanical Engineering Department, Ben-Gurion University of the Negev, Beer-Sheva, Israel.
- BAR-COHEN, A., RUDER, Z. & GRIFFITH, P. 1984 Thermal and hydrodynamic phenomena in a horizontal, uniformly heated steam generating pipe. In *HTD: Vol. 34, Basic Aspects of Two-Phase Flow and Heat Transfer*. ASME, New York.
- BAR-COHEN, A., RUDER, Z. & GRIFFITH, P. 1986 Development and validation of boundaries for circumferential isothermality in horizontal boiler tubes. *Int. J. Multiphase Flow* **12**, 63–77.
- CHANDRAN, R., CHEN, J. C. & STAUB, F. W. 1979 Local heat transfer coefficients around horizontal tubes in fluidized beds. ASME Publication No. 79-HT-75.
- RUDER, Z. 1984 The influence of two-phase flow regimes on circumferential temperature distribution in horizontal, steam generating tubes. Ph.D. Thesis, Department of Mechanical Engineering, Ben-Gurion University of the Negev, Beer-Sheva, Israel.
- RUDER, Z., BAR-COHEN, A. & GRIFFITH, P. 1984 Major parametric effects on isothermality in horizontal steam generating tubes. *AIChE J*
- WEISMAN, J., DUNKAN, D., GIBSON, J. & CRAWFORD, T. 1979 Effects of fluid properties and pipe diameter on two-phase flow patterns in horizontal lines. *Int. J. Multiphase Flow* **5**, 436–462.